10-2010

Facile Pyrolytic Synthesis of Silicon Nanowires

Joo C. Chan
Intel

Hoang Tran
Portland State University

James W. Pattison
Army Research Laboratory

Shankar B. Rananavare
Portland State University

Published in final edited form as:
Solid State Electron. 2010 October 1; 54(10): 1185–1191. doi:10.1016/j.sse.2010.05.011.

Facile Pyrolytic Synthesis of Silicon Nanowires

Joo C. Chan[a], **Hoang Tran**[b], **James W. Pattison**[c], and **Shankar B. Rananavare**[*,b]

James W. Pattison: james.pattison1@arl.army.mil

[a] Advanced Logic Components, Ronler Acres, Intel, Hillsboro, OR 97123

[b] Portland State University, Chemistry Department, USA

[c] Army Research Laboratory, USA

Abstract

One-dimensional nanostructures such as silicon nanowires (SiNW) are attractive candidates for low power density electronic and optoelectronic devices including sensors. A new simple method for SiNW bulk synthesis[1,2] is demonstrated in this work, which is inexpensive and uses low toxicity materials, thereby offering a safe, energy efficient and green approach. The method uses low flammability liquid phenylsilanes, offering a safer avenue for SiNW growth compared with using silane gas. A novel, duo-chamber glass vessel is used to create a low-pressure environment where SiNWs are grown through vapor-liquid-solid mechanism using gold nanoparticles as a catalyst. The catalyst decomposes silicon precursor vapors of diphenylsilane and triphenylsilane and precipitates single crystal SiNWs, which appear to grow parallel to the substrate surface. This opens up possibilities for synthesizing nano-junctions amongst wires which is important for the grid architecture of nanoelectronics proposed by Likharev[3]. Even bulk synthesis of SiNW is feasible using sacrificial substrates such as $CaCO_3$ that can be dissolved post-synthesis. Furthermore, by dissolving appropriate dopants in liquid diphenylsilane, a controlled doping of the nanowires is realized without the use of toxic gases and expensive mass flow controllers. Upon boron doping, we observe a characteristic red shift in photoluminescence spectra. In summary, an inexpensive and versatile method for SiNW is presented that makes these exotic materials available to any lab at low cost.

Keywords

Silicon nanowires; dopants; photoluminescence; gold nanoparticles; HR-TEM

Introduction

Currently, silicon nanowires are the subject of significant resurgent interest in nanoelectronics[4], optoelectronics[5] and in solar energy[6] owing to their coherent transport[7] of charge carriers and due to observations of photo[8] and electroluminescence[9] from them. As the CMOS scaling leads to the transistor gate dimensions of 20-30nm in length, quantum phenomena such as tunneling degrade on to off current ratios. The associated leakage current increases the device operational temperature, requiring expensive onboard cooling strategies. A radically different approach to the next

[*]Corresponding author. Tel.: 1-503-725-8511; fax: 1-503-725-9525. ranavas@pdx.edu (S. B. Rananavare).

stage of nanoelectronics has been pursued, including a notion of grid architecture[3] applicable to nanowire/nanotube components. Using these 1-D components, bottom up assembly methods have been applied to construct logic devices such as inverter, SRAM, ring oscillators[10-12] etc. A further set of electronic applications of SiNW is in their use for solar-energy [6,13-16] conversion, exploiting photon induced charge separation at their PN junctions. In addition SiNWs have found their way to sensor applications, since the surface of silicon/silicon oxide is easily derivatized[17-20]. A popular modality of sensing utilizes changes in the threshold voltage of MOS transistors[21]. By measuring the shift in the transistor gate voltage, femto-molar DNA (polyanion) concentrations have been detected.

However, these promising materials remain difficult to synthesize on a bulk scale. Standard synthesis methods include chemical vapor deposition[22,23], laser ablation[24-26], microwave[27,28] or oxide assisted growth[1,29-34]. Such methods often lead to small yields of SiNWs, unfortunately accompanied by variable thickness of native oxide capping them. Although supercritical fluid [35-37] and colloidal solution methods[38] for bulk synthesis have been developed, some of them employ flammable organic solvents and require high (>200atm) pressure and >400C operational conditions that make up-scaling a challenging task, requiring the use of titanium reactors.

The three most commonly observed growth mechanisms for SiNWs are: vapor-liquid-solid(VLS)[22], vapor-solid-solid (VSS)[39] and oxide assisted[30,34,40,41] growth. The VLS mechanism that was proposed by Wagner and Ellis[22] in 1964, suggests that a properly chosen metal catalyst first decomposes a silicon precursor molecule and dissolves liberated silicon in a liquefied eutectic drop of the catalyst-metal-silicon. Above the saturation limit of such a nano-droplet, the excess silicon is extruded in the form of a SiNW. The VLS mechanism is generally controlled by the synthesis/growth temperatures (i.e., corresponding to eutectic temperatures and above for a given metal-silicon combination) and the terminal location of the metal catalyst at the growing tip of SiNW. Givargizov[42] and Westwater[23] et al further clarified the elemental steps involved in the growth process and have concluded that the super-saturation of the Si-catalyst controls the effective diameter of the Si-NW. In cases of rapid growth, e.g., laser ablation, the size of the catalyst is believed to control the diameter of the SiNW[43]. In a VSS mechanism, the catalyst remains solid and the growth of SiNWs presumably takes place through an accretion of surface-diffusing Si atoms into NWs. In the oxide assisted growth, it is believed that non-stoichiometric Si sub oxides are molten and direct the growth of NWs. The advantage here is that no catalyst is needed, and even SiO heating can produce the SiNW. This method is capable of producing large quantities of SiNW. The only drawback of the method is that growth conditions require high temperatures ≈ 1100°Cwhich limits the application of these nanowires for bottom up fabrication as the precise control over positioning of SiNW during growth at such a high temperature is difficult to realize.

The method presented herein differs drastically from others in that no reactive silicon precursor flows over the catalysts, but rather forms a stagnant vapor over the reactive catalysts. The liquid form of silicon precursor used allows doping through dissolution of appropriate organic compounds. Much like other methods that utilize CVD reactors for VLS growth, this technique allows growth on any substrate capable of withstanding Au-Si eutectic temperatures. We have been able to exploit this feature to grow SiNW on $CaCO_3$ (ordinary chalk), aluminum and glass wool. After synthesis substrate can be dissolved using acid solutions, thus enabling a bulk synthesis of SiNWs.

Experimental methods

A. Chemical reagents

All chemical were used as arrived. List of chemical reagents: $AuCl_3$ (STREM CHEMICALS; CAS No. 13453-07-1, Lot# 141380-S1, gold(III) chloride, 99%); 1,8-octanediol (98%, Sigma-Aldrich, Cat. No. O-330-3, CAS No. 629-41-4); dimethyl formamide (Sigma-Aldrich, Cat. No. 319937, CAS No. 68-12-2, >99.8%); sodium borohydride (Sigma-Aldrich, Cat. No. 452882, CAS No. 16940-66-2, powder, >98.5%); diphenylsilane (Sigma-Aldrich, Cat. No. 14,848-2, CAS No. 775-12-2, 97%); triphenylborane (Sigma-Aldrich, Cat. No. T82201, CAS no. 960-71-4, powder, <2% H_2O). Household chalk and glass wool as well as aluminum thin films deposited on Si wafers were also used as substrates for SiNW growth.

B. Gold catalyst nanoparticle synthesis and deposition

Gold nanoparticles were synthesized in an nonaqueous solvent/surfactant system composed of dimethyl formamide (DMF) and 1,8-octanediol which is a bolaamphiphile (i.e., a surfactant molecule containing two hydrophilic groups at both termini[44,45]). Higher gold nanoparticle concentration could be generated in DMF solutions than in water due to higher solubility of 1,8-octanediol in the former. The bolaamphiphiles such as 1,8 -octanediol tend to self-assemble into monomolecular discs rather than spherical micelles in aqueous as well as nonaqueous solvents [1,44]. The gold (III) chloride (100 μmols $AuCl_3$ per liter of DMF) solution was prepared with 1,8-octanediol (0.34 M) solution and reduced with freshly prepared 0.27 M $NaBH_4$. For TEM studies as well as SiNW synthesis these particles were deposited on TEM grid or substrates and dried by baking them at 100 °C for 30 minutes in an N_2 environment. The resulting nanoparticle size was about 5 nm as determined by AFM height analysis (not shown) as well as analysis of TEM data shown in Figure 1. Significant asymmetry in the nanoparticle shape could arise from their growth and nucleation on the both faces of the hydrophilic head-group regions of the surfactant monolayer as shown schematically in the inset. This synthetic approach is different from traditional syntheses in reverse micellar phase[46] of normal (only one hydrophilic group) surfactants; the latter generally leads to spherical particles directed by spherical shape of the aqueous micellar core in reverse micelles.

C. Synthesis of SiNWs using duo chamber glass tube

Diphenylsilane was first pipetted into the bottom of a borosilicate glass tube (0.8 cm O.D. × 0.6 cm I.D.), ensuring that the solution did not adhere to the sidewalls. The tube was sectioned into two chambers by thinning to a neck with a propane torch at approximately 5 cm from the bottom of the tube. The catalytic nanoparticle coated substrate was then inserted into the tube. The thinned neck prevents the substrate from falling into the DPS. The top of the tube was thinned to a neck with a propane torch approximately 13 cm from the bottom of the tube for ease of sealing. The reagent (DPS) was de-oxygenated via the freeze-pump-thaw method on a glass vacuum line at pressure of 100 mTorr till no more gas evolution was observed from liquid DPS. After evacuation, the glass tube was sealed off resulting in a duo-chamber glass reaction vessel as shown in Figure 2.

To ensure that the substrate reaches the desired temperature before the reaction, the substrate chamber end was inserted into the preheated core (at the preset temperature), leaving the DPS chamber outside of the Lindberg tube furnace. The sample glass tube was maintained at that location for a minimum of 5-7 minutes before fully inserting it into the heated region of the furnace. For doped SiNW synthesis, triphenylborane was dissolved directly into DPS. The resulting nanowires were transferred from the silicon wafer substrate surface to TEM grid by rubbing, while for SEM studies such transfer was not necessary.

D. Electron microscopy

An FEI Siron XL30 model SEM was used for electron microscopy imaging. Imaging was performed at an accelerating voltage of 5 kV at beam current of ~300 μA.

TEM was used for bright field, dark field, selected area diffraction, EDX analysis and high resolution lattice plane imaging. The TEM microscope used was a FEI Technai F-20 TEM (PSU electron microscopy center). Imaging was performed at an accelerating voltage of 200 kV. A column vacuum of less than 0.10 μtorr was achieved. In many instances we simply used the TEM grid as a substrate for the catalyst and carried out growth of SiNW directly on the grid. The results of such study appear TEM data appear in Figure 3.

Nanowires synthesized on the sacrificial substrate of $CaCO_3$ were sputter coated with thin layer of gold to prevent sample charging. Samples prepared on silicon wafers or borosilicate glass did not require gold sputtering.

E. Photoluminescence spectroscopy

The optical photoluminescence (PL) of the doped and the undoped SiNWs was characterized on a Shimadzu spectrofluorophotometer RF-5301PC, using a xenon light source and 3 nm bandwidth. For these studies, SiNWs were dispersed in degassed chloroform (freshly opened HPLC grade $CHCl_3$) by ultrasonicating the SiNW bearing substrates.

F. Photolithographic patterning

Silicon wafer coated with evaporated 40nm thick aluminum (by thermal evaporation) film was patterned using an i-line aligner (Tamarack Scientific Co, Inc., Model 162A) and Shipley positive resist (SPR version 220-3). The process flow is as given below.

1. Spin coat SPR 220-3 resist @ 2000rpm for two minutes
2. Pre-bake @ 115 °C for 90sec
3. Exposure @ 250mJ/cm^2
4. Post exposure bake @ 115°C for 90sec
5. Resist develop with 0.27M NaOH for 18sec
6. Post develop bake @ 114°C for 70sec.
7. Al Etch with 0.07M NaOH @ 43°C for 60se

Once crafted, a drop (5ul) of nanoparticle catalyst suspension was placed in the trench and dried, followed by the synthetic procedure outlined above.

Results

A. VLS growth mechanism

The drop-like tip shape of the nanowires terminus as seen in Figure 3 suggests a VLS mechanism of growth. The observed SiNW tip composition indicated the presence of Au, as shown in the EDX analysis (the rightmost panel).

One of the remarkable features of these wires is that they tend to grow parallel to the substrate surface, especially in trenches. This is clearly apparent in Figure 4 below, which shows an SEM image of a SiNW as grown on a rough planar borosilicate glass surface. HR-TEM data shown revealed that the most common direction of growth is along [110] plane for sub 30nm diameter SiNWs while for 100nm nanowires growth along [111] and [100]

planes was more common. These assignments were made using a calculator at BYU EE dept website[47]. SiNWs were typically covered by oxide layers a few nanometers thick presumably formed upon exposing the SiNWs to ambient conditions after synthesis, although it is possible that some adventitious oxygen could be present or released during the high temperature synthesis that produces the observed thin oxide layer. See below

B. Doping and Photoluminescence

Boron doped nanowires were synthesized using various levels of triphenyl borane in diphenyl silane. The optical photoluminescence (PL) of the doped and the undoped SiNWs exhibit (Figure 5) optical emission from SiO_x in 350-450 nm region [8,16,48-50] and a commonly observed red-emission due to Si at about 700 nm in Si nanocrystals [51] and nanowires[8]. Specifically, the origins of emission in the 400 nm range has been ascribed to neutral oxygen vacancy[50] and also to the $T_1 \rightarrow S_0$ transition of the twofold coordinated Si in SiO_2[52](_O–Si–O). An alternate explanation of 350 nm and 415 emission bands in undoped and in highly doped samples is that they are associated with the reformation Si-Si and Si-B bonds after photo-excitation, based on bond formation enthalpies. The weak peak at 415 nm corresponds approximately to the Si-B bond enthalpy[53] and the stronger peak at 357 nm to the Si-Si bond enthalpy. The 415 nm band is not resolved in the undoped samples which is consistent with the above explanation. Nonetheless, it should be borne in mind that these spectra were taken immediately after SiNW synthesis. In such samples, the oxide layer thickness is small (less than 2 nms for SiNW with diameters varying between 20-100nms), therefore fluorescence contribution (at 400-450nm) from SiO_x is likely to be small.

The results in Figure 5B, showed a small red shift in the emission at 685 nm upon doping; it progressively increased with the dopant concentration. At the highest level of dopant concentration used during synthesis (7.5 mole %), the emission pattern was characterized by high intensity and a complex lineshape, perhaps resulting from a superposition of multiple emission bands. No further quantitative analysis of this complex lineshape was performed. Qualitatively, however, these results are similar to those reported for doped silicon nanoparticles by Sato et al[51]. The maximum measured magnitude of the PL red shift, for the 685 nm red emission, was 20 nm. This suggests that a maximum of 0.4% boron insertion in the bulk of SiNWs based on the results Sato et al [51]. Thus, large concentration of dopant employed during the synthesis did not translate into an equivalent concentration of inserted dopants in SiNWs. This result is similar to sol-gel synthesis of doped oxide semiconductors, wherein we found only a small fraction of dopant incorporates into crystalline lattice[54, 55] of an oxide semiconductor despite its large concentration used during synthesis. SEM data, not shown here, also showed an increased propensity towards formation of abrupt bends in SiNWs as the concentration of dopant was increased. These data, therefore, suggest an insertion of B dopant into silicon lattice (also see the discussion section below) which we plan to confirm later through electrical characterization.

PL of as grown SiNWs on a silicon wafer and a copper grid was measured using a reflective fluorescence microscope; the results, as shown in Figure 6, corroborated the solution phase PL data.

C. Bulk Synthesis

Our approach, as discussed above, is to use a sacrificial high surface area substrate that can be dissolved after synthesis. One can use high surface area powders and larger inter-substrate spacing provided by fibrous materials such as glass wool to achieve bulk synthesis. Figure 7 shows SiNWs grown on a $CaCO_3$ powder (chalk) substrate that is readily dissolved using dilute hydrochloric acid. Note that our reaction chamber contains stagnant vapors of silicon precursor which permeates through the powder matrix and permits growth

throughout the connected porous matrix. A similar synthesis of SiNWs on glass wool appears in Figure 7, where we observe a surface parallel growth of SiNWs as seen in Figure 4. In this case, glass wool can be dissolved by treating it with buffered hydrofluoric acid.

Discussion

In any synthetic method deployed to produce SiNWs, several important features are desirable. They include size control (length and diameter), ease of doping, and surface parallel growth. We discuss these issues in the context of device applications of SiNWs for a catalyst directed VLS-type growth.

A. Size control

At currently realized sizes of planar CMOS devices, with transistor gate lengths approaching sub 25nm scale, it is desirable to synthesize SiNWs of smaller diameter to provide high packing density devices on a grid architecture[3]. A common perception is that the size of catalyst/silicon droplet controls the dimension of the NW. Although intuitively appealing, the results of Givargizov [42], Westwater[23], and Sunkara[28] suggest that the degree of silicon super-saturation in the eutectic catalyst may play an even bigger role. We studied the SiNW diameter by systematically varying the silicon precursor concentration in reaction glass tube, thereby modulating the degree of supersaturation in the AuSi eutectic nano-droplet. Following Givargizov, we write

$$d \simeq d_c \simeq \frac{4\Omega\gamma_{LV}}{k_B T \ln x} \quad (1)$$

Where $x = s/s_0$ is a measure of super-saturation and S is proportional to gas phase concentration of silicon, γ_{LV} the specific surface energy and Ω is the atomic volume of silicon. For determination of diameter we used at least 15-20 SiNWs from a single SEM image; the resulting standard deviations were about 10-20% of the mean diameter. This distribution was averaged with data from three separate syntheses conducted under identical conditions.

The deviation of mean nanowire diameters from different syntheses was larger than expected from the standard deviation extracted from analysis of any single SEM image. Uncertainty in determining the internal volume of the manually sealed glass tubes (Figure 2) also adds to error in determining S, the vapor phase concentration of Si; although its log dependence suppresses its overall contribution to the evaluation of parameters from equation 1. These statistics can be improved with larger volume glass vessels with a better temperature controlled furnace. A plot of 1/d vs. ln(S) is shown above. The best fit slope of straight line is $10^7\ m^{-1}$, which is within an order of magnitude of the estimated slope ($k_bT/(4\Omega\gamma_{LV}) = 7.8 \times 10^7\ m^{-1}$ (using $\Omega = \frac{2 \times 10^{-29} m^3}{1\ atom\ Si}$; $\gamma_{LV} = 1600\ mN/m$, and $T = 723\ K$). Data in Figure 8 qualitatively support the supersaturation/nucleation model. Alternatively, given that gold nanoparticles synthesized from the same batch were used in these set of syntheses, the observation of concentration independent diameters would have lent support to the notion that the catalyst size controls the NW diameter. Nevertheless, it should be noted that the observed larger diameters (20-100 nm) of SiNWs compared with the size of Au nanoparticles (5-10) could be a result of a diffusion controlled aggregation of gold nanoparticles followed by fusion of the diffusing nano-droplets of Au-Si formed at eutectic temperature. Even in Figure 1, where gold nanoparticles were deposited from a volatile solvent, such incipient aggregation at room temperature is apparent. Although this fusion

mechanism explains the larger diameter of NWs, it does not account for the SiNW diameter dependence on the Si precursor concentration. Further studies using a lower concentration of Au nanoparticles or their isolation/anchoring on a substrate to prevent inter-particle coalescence are needed to confirm this latter hypothesis. Although the diameter of the as grown SiNWs can be thinned using Si oxidation/HF etching cycles, it would be desirable to control both DPS super-saturation and isolation of gold nanoparticles, especially for bulk nanowire synthesis.

The length of nanowires depended[43] on the reaction time as long as the entire precursor was not used up. Our studies have shown that it is possible to grow SiNW longer than 15 μm within 7 minutes of growth time[1]; thus growth under these conditions is very rapid, approaching 2-4 μm/min. Generally, we have employed growth conditions of much longer duration where all the DPS is consumed. The resulting nanowires are very long and entangled making evaluation of length distribution difficult from SEM images. Another approach to controlling the length of the nanowires is through changing relative ratio of DPS/Au nanoparticle if nanoparticle fusion can be avoided by anchoring them to the substrate.

B. Doping

Our synthesis method permits SiNW doping by choosing nonvolatile dopant mixed with silicon precursor which is highly desirable for their ultimate application in nanoelectronics. We have used solids[1] that are soluble in DPS such as triphenyl borane (p-type dopant) or diphenyl phosphine (n-type) for doping. The advantage of using solid dopants is that it eliminates the expensive and toxic gas handling issues associated with B_2H_6 and PH_3. Other researchers have taken this latter approach, following the standard practices in the semiconductor industry[56]. However, doping in nanostructures is likely to be a complex issue owing to a larger proportion of surface atoms than the conventional planar structures (wafers). As mentioned before, we found that the dopant species preferred to partition between the surface and the bulk regions of nanostructures[54,55]. A recent CV measurement study of Garnett et al[57] on doped SiNW also suggests a radially nonuniform dopant distribution profile with higher concentration of dopants located near the Si-SiO_2 interfacial region. This is unfortunate as the progressive surface oxidation of SiNW could lead to a time dependent depletion of carrier concentration unless the SiNW surface is passivated. An extreme example of boron doped SiNWs samples stored over two years is shown in Figure 9. It shows a much thicker oxide layer (≈8 nm) as compared to HR-TEM studies of immediate (<2weeks) post synthesis samples showing very thin oxide layer thickness (<3 nm, not shown). We have studied this kinetics of oxide growth at room temperature over a period of three years; these results will be presented elsewhere.

The low magnitude of red shifts observed in Figure 5B suggested a low degree of doping and one would not expect to observe a high concentration of Si-B bonds as we implied from the low wavelength emission (Figure 5A) of corresponding Si-B bonds. Nonetheless, if the boron distribution is peaked near the interface of SiO_x and Si and not in the bulk Si, then the observed intensity of Si-B peak can be rationalized. It is also consistent with the complex emission pattern observed at higher of doping in the red region of the spectrum; see Figure 5B. Nevertheless, a radial dopant distribution across our nanowires, as synthesized by our new method, is undetermined at present. Future electrical characterization studies are planned to investigate the dopant profile.

C. Horizontal Growth

As can be seen in the SEM images of Figures 4 & 7, the growth of nanowires appears to run parallel to surface. This is a distinctive feature of our closed reactor system. It is generally

accepted that the VLS growth mechanisms gives rise to surface normal growth of SiNWs. However, it should be borne in mind that these studies utilized flow reactors wherein a surface normal positive concentration gradient prevails. On the contrary, in our reaction vessel there is no flow of reactants. Stagnant vapors of the precursors would be expected to create a multilayer adsorption, i.e., a negative surface normal gradient. For growing Si-Au catalytic droplets there is ample availability of Si precursor species on the substrate surface. We suggest that these conditions lead to the observed surface parallel growth; although the precise origins of this growth mode are presently unknown. Potentially such surface parallel growth is desirable, if in-situ growth of SiNWs in devices is needed. Shown in Figure 10 is a preliminary proof of concept study of optical lithographically patterned aluminized (40 nm thick) silicon wafer, where the SiNWs were grown in the lithographically exposed trenches. Because either the gold nanoparticles accumulated at the Al-Si step or Al helped catalyze the growth of nanowires, we observed a large number SiNWs at the edge, some which run parallel to surface to connect the two electrodes. Further optimization of synthetic conditions for detailed electrical characterization studies is underway. It should be noted that by carrying out the synthesis near the melting point of Aluminum it would be possible to *synthesize* SiNW electrode contacts. To realize this goal it is essential to eliminate oxygen during synthesis to prevent formation of aluminum silicates. An approach to removing oxygen is by introducing sacrificial, easily oxidized organic compounds such as ascorbic acid to trap oxygen into CO/CO_2 gases before silicon/gold or silicon/aluminum eutectic temperature is reached.

An important key step in realizing grid architecture on a large scale is to prepare fused junction amongst SiNWs *during the SiNW synthesis*. Synthesis of junction is possible by directing NW growth in prefabricated channels. Such directed growth allows parallel processing of the junctions. We have observed formation of such junctions[1] on our substrates and their characterization will be presented elsewhere.

In summary, a simple, scalable and inexpensive method for doped and undoped silicon nanowire synthesis is presented. The growth mechanism of the SiNW in such closed reaction chambers appears to be VLS-like with one significant difference: a surface parallel growth of nanowires. Such mode of growth could be valuable in top-down crafting of grid-architecture of nanowires. Our method also permits synthesis of bulk quantities of SiNWs useful for bottom up assembly methods in developing chemical sensors, flexible solar cells based on SiNWs.

Acknowledgments

Many stimulating conversations with Professor Marvin Silverberg are gratefully acknowledged. Authors thank Prof. Andrea Goforth and Prof. Scott Reed for allowing generous use of their spectrofluorometers. We also wish to thank Dr. Marilyn Mackiewicz (Fluorescence) and Dr. Timothy Gutu (HR-TEM) for technical assistance. We are indebted to Professor John Freeouf for providing the use of a fluorescence microscope.

References

1. Chan, JC. Ph D (Thesis). Chemistry Department, Portland State University; Portland: 2008.
2. Chan J, Tran H, Rananavare SB. Nanotechnology. 2010 to be submitted.
3. Likharev, KK. Device Research Conference, 2007 65th Annual; 2007. p. 9
4. Lieber CM, Cui Y. Science 2001;291:851. [PubMed: 11157160]
5. Brus L. J Phys Chem 1994;98/14:3575.
6. Tsakalakos L, Balch J, Fronheiser J, Korevaar BA, Sulima O, Rand J. Applied Physics Letters 2007;91/23:233117.
7. Zhong Z, Fang Y, Lu W, Lieber CM. Nano Lett 2005;5/6:1143. [PubMed: 15943458]

8. Zeng XB, Liao XB, Wang B, Dai ST, Xu YY, Xiang XB, Hu ZH, Diao HW, Kong GL. Journal of Crystal Growth 2004;265:94.
9. Solanki R, Huo J, Freeouf JL, Carruthers JR. Nanotechnology 2004;15:1848.
10. Lieber CM, Huang Y, Duan X, Wei Q. Science 2001;291:630. [PubMed: 11158671]
11. Bachtold A, Hadley P, Nakanishi T, Dekker C. Science 2001;294/5545:1317. [PubMed: 11588220]
12. Avouris P, Derycke V, Martel R, Appenzeller J. Nano Letters 2001;1/9:453.
13. Jeon M, Kamisako K. Materials Letters 2009;63/9-10:777.
14. Sivakov V, AndrÃ¤ G, Gawlik A, Berger A, Plentz J, Falk F, Christiansen SH. Nano Letters 2009;9/4:1549. [PubMed: 19281253]
15. Tian B, Zheng X, Kempa TJ, Fang Y, Yu N, Yu G, Huang J, Lieber CM. Nature 2007;449/7164:885. [PubMed: 17943126]
16. Hu L, Chen G. Nano Letters 2007;7/11:3249. [PubMed: 17927257]
17. Stewart MP, Buriak JM. Advanced Materials 2000;12/12:859.
18. Buriak JM. Philosophical Transactions of the Royal Society A: Mathematical, Physical and Engineering Sciences. 2006;364/1838:217.
19. Chen W, Yao H, Tzang CH, Zhu J, Yang M, Lee ST. Appl Phys Lett 2006;88/21:213104.
20. Elibol OH, Morisette D, Akin D, Denton JP, Bashir R. Applied Physics Letters 2003;83/22:4613.
21. Wu CC, Ko FH, Yang YS, Hsia DL, Lee BS, Su TS. Biosensors and Bioelectronics 2009;25/4:820. [PubMed: 19765969]
22. Wagner RS, Ellis WC. Appl Phys Lett 1964;4/5:89.
23. Westwater J, Gosain DP, Tomiya S, Usui S. J of Vac Sci Tech B 1997;15/3:554.
24. Fukata N, Matsushita S, Tsurui T, Chen J, Sekiguchi T, Uchida N, Murakami K. Physica B: Condensed Matter 2007;401-402:523.
25. Lieber CM, Morales AM. Science 1998;279:208. [PubMed: 9422689]
26. Lee ST, Zhang YF, Tang YH, Wang N, Yu DP, Lee CS, Bello I. Applied Physics Letters 1998;72/15:1835.
27. Sharma S, Sunkara MK. Nanotechnology 2004;15/1:130.
28. S S, Sunkara MK, Miranda R, Lian G, Dickey EC. Appl Phys Lett 2001;79/10:1546.
29. Gole JL, Stout JD, Raunch WL, Wang ZL. Applied Physics Letters 2000;76/17
30. Jianfeng Z, Min H, Minda L, Fengqi S, Jianguo W, Yanfeng C, Guanghou W. J of Cryst Growth 2004;269/2-4:207.
31. Lee ST, Wang N, Tang YH, Zhang YF, Lee CS. Phys Rev B 1998;58/24:R16024.
32. Lee ST, Wang N, Zhang YF, Tang YH, Lee CS. Applied Physics Letters 1998;73/26:3902.
33. Park BT, Yong K. Nanotechnology 2004;15/6:S365.
34. Zhang RQ, Lifshitz Y, Lee ST. Advanced Materials 2003;15/7-8:635.
35. Korgel BA, Holmes JD, Johnston KP, Doty RC. Science 2000;287:1471. [PubMed: 10688792]
36. Korgel BA, Lu X, Hanrath T, Johnston KP. Nano Letts 2003;3/1:93.
37. Korgel BA, Shah PS, Hanrath T, Johnston KP. J Phys Chem B 2004;108:9574.
38. Heitsch AT, Fanfair DD, Tuan HY, Korgel BA. Journal of the American Chemical Society 2008;130/16:5436. [PubMed: 18373344]
39. Wang Y, Schmidt V, Senz S, Gosele U. Nature Nanotechnology 2006;1/3:186.
40. Zhang RQ, Chu TS, Cheung HF, Wang N, Lee ST. Material science and engineering C 2001;16:31.
41. Yao Y, Li F, Lee ST. Chemical Physics Letters 2005;406/4-6:381.
42. Givargizov EI. J of Cryst Growth 1975;31:20.
43. Lieber CM, Cui Y, Lauhon LJ, Gudiksen MS, Wang J. Appl Phys Letts 2001;78/15:2214.
44. Thompson DH, Wong KF, Humphry-Baker R, Wheeler JJ, Kim JM, Rananavare SB. Journal of the American Chemical Society 1992;114/23:9035.
45. Di Meglio C, Rananavare SB, Svenson S, Thompson DH. Langmuir 2000;16/1:128.

46. Wong, EW.; Sheeleigh, C.; Rananavare, SB. Structured Studies of Catalytic Nanoparticles. Oakridge National Laboratory; Oak Ridge: 1992.
47. Provo, Utah: 2008. “Angle Between Planes” calculator from Brigham Young University, Department of Electrical and Computer Engineering. website (http://www.ee.byu.edu/cleanroom/EW_orientation.phtml)
48. Bhattacharya S, Banerjee D, Adu KW, Samui S, Bhattacharyya S. Applied Physics Letters 2004;85/11:2008.
49. Colli A, Hofmann S, Fasoli A, Ferrari AC, Ducati C, Dunin-Borkowski RE, Robertson J. Applied Physics A: Materials Science & Processing 2006;85/3:247.
50. Wang YW, Liang CH, Meng GW, Peng XS, Zhang LD. Journal of Materials Chemistry 2002;12/3:651.
51. Sato K, Niino N, Fukata N, K H, Yamauchi Y. Nanotechnology 2009;20:60.
52. Brewer A, Haeften Kv. Applied Physics Letters 2009;94/26:261102.
53. <http://www.webelements.com/silicon/bond_enthalpies.html>.
54. Chaparadza A, Rananavare SB, Shutthanandan V. Materials Chemistry and Physics 2007;102/2-3:176.
55. Chaparadza A, Rananavare SB. Nanotechnology 2010;21/3:035708. [PubMed: 19966386]
56. Glang R, Kippenhan BW. IBM J of Res and Dev 1960;8:299.
57. Garnett EC, Tseng YC, Khanal DR, Wu J, Bokor J, Yang P. Nature Nanotechnology 2009;4:311.

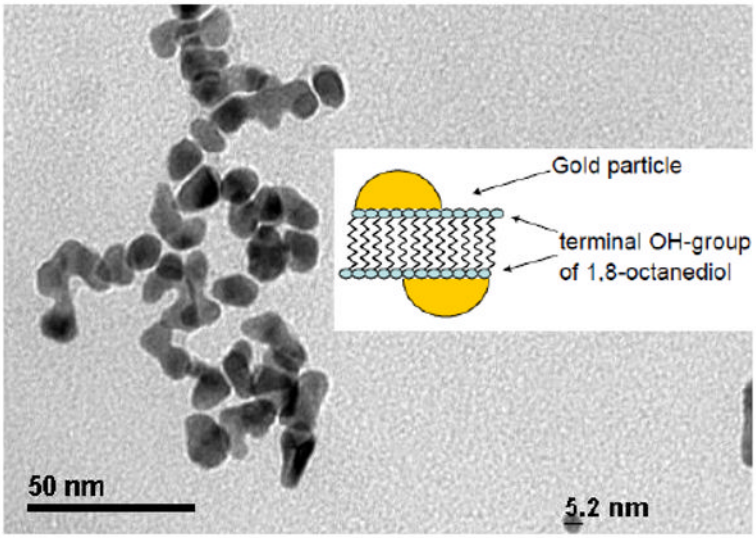

Figure 1.
Gold nanoparticles used to catalyze SiNW Growth. TEM data were collected using Holey carbon TEM grids on FEI Tecnai F-20 microscope operating at 200 kV. The inset depicts potential growth mechanism for gold nanoparticles on the both surfaces of the bolaamphiphile,1,8-octanediol.

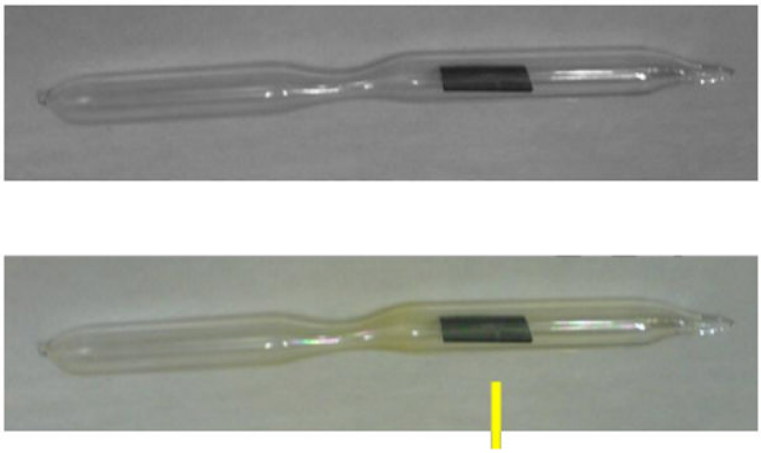

Figure 2.
Sealed glass tube synthesis of SiNW. Top (before) and bottom (after) synthesis. The DPS and substrate chambers are located in two different regions separated by a narrow passage in the center.

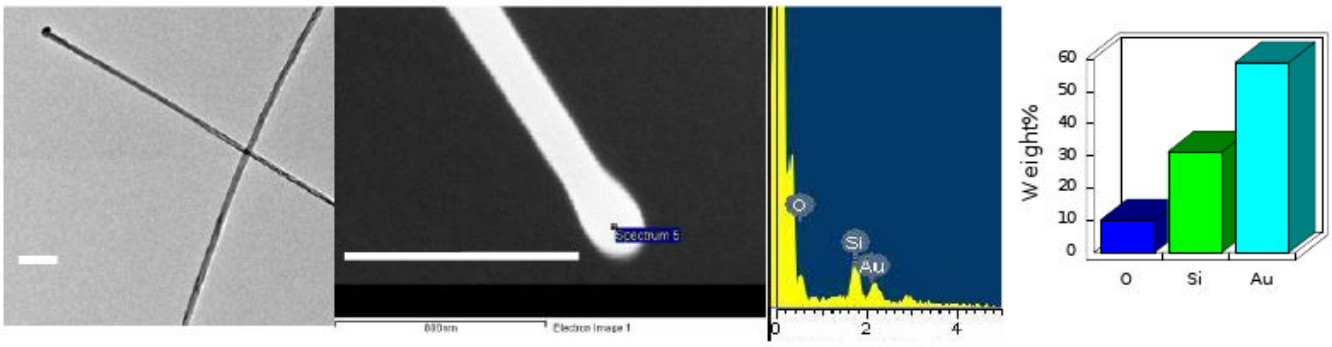

Figure 3.
VLS mechanism of growth of SiNW. TEM (left) and SEM (right) of SiNW tip bearing gold eutectic. To the right are EDX and elemental analysis chart. Scale bars correspond to 1 μm length. For this study SiNWs were directly grown of the surface of the TEM grid thereby avoiding mechanical transfer of SiNW to grid.

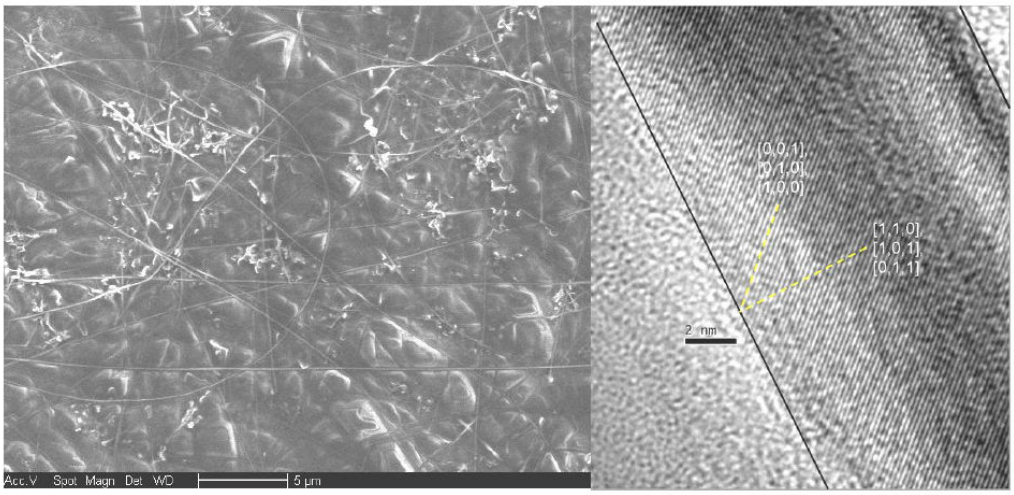

Figure 4.
SEM image to the left illustrates (a) Surface parallel growth of SiNW (b) HR-TEM data shows 100 1attice planes indicated by the dashed yellow line. The grooves were not patterned; they were characteristics of the glass substrate used. A clear separation of lattice fringes and amorphous oxide on the surface of the SiNW is observed. The SiNW growth direction is at 45 degree angle and hence the corresponding miller indices would be [1,1,0], [1,0,1] etc (see text).

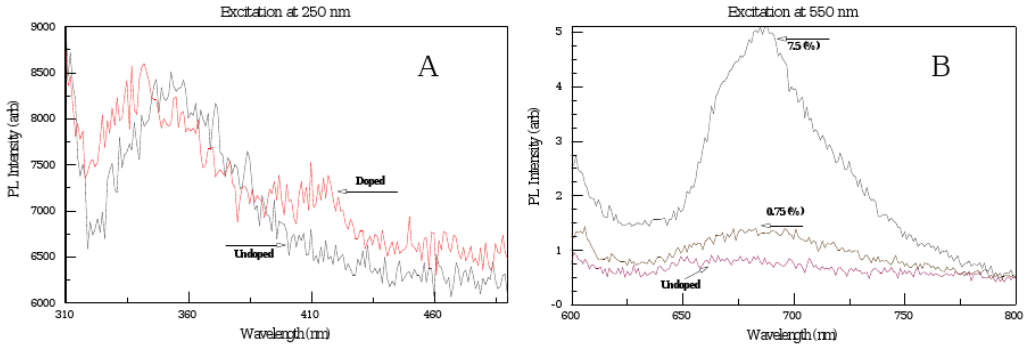

Figure 5.
PL spectra from un-doped and boron doped SiNWs A) excitation wavelength 250nm B) excitation wavelength 550 nm.

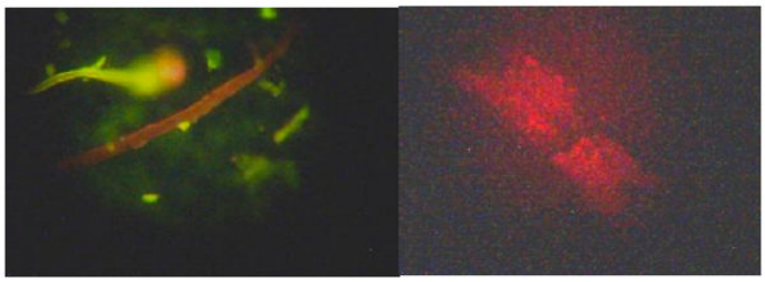

Figure 6.
Photoluminescence microscopy of nanowires deposited on copper (left) and silicon (right) substrates. Excitation wavelength was 450-500nm; emission was observed in 510-800nm. Magnifications 40×.

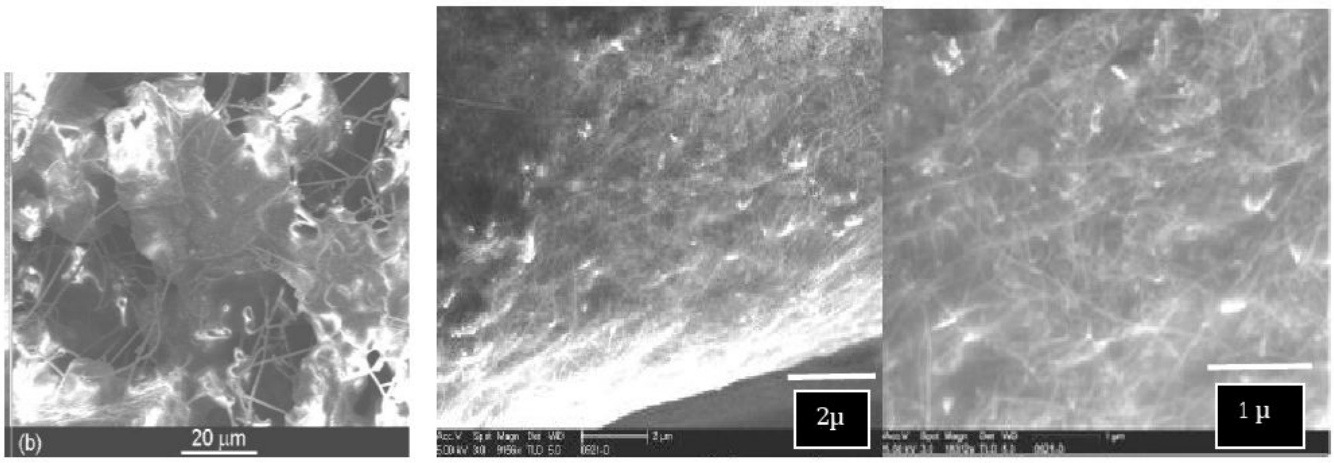

Figure 7.
SEM images of SiNW growth on powdered $CaCO_3$ (left) and on glass wool (middle and right). Small fraction of material (either chalk powder or glass wool) was dipped in solvent suspended gold nanoparticles followed by drying at 100C in the N_2 environment before transferring in reaction vessel.

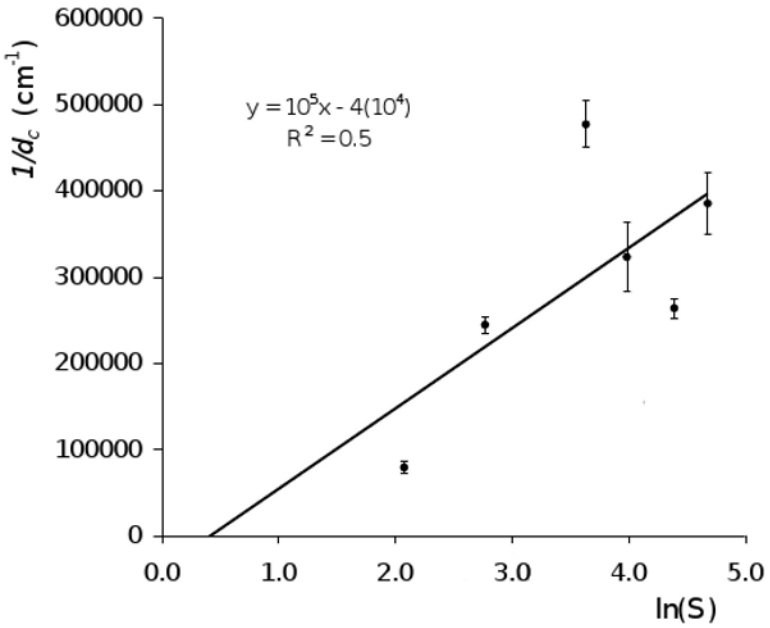

Figure 8.
Plot of 1/NW diameter versus DPS concentration. Error bars were determined from average of three separate syntheses and included at least 50 SiNWs.

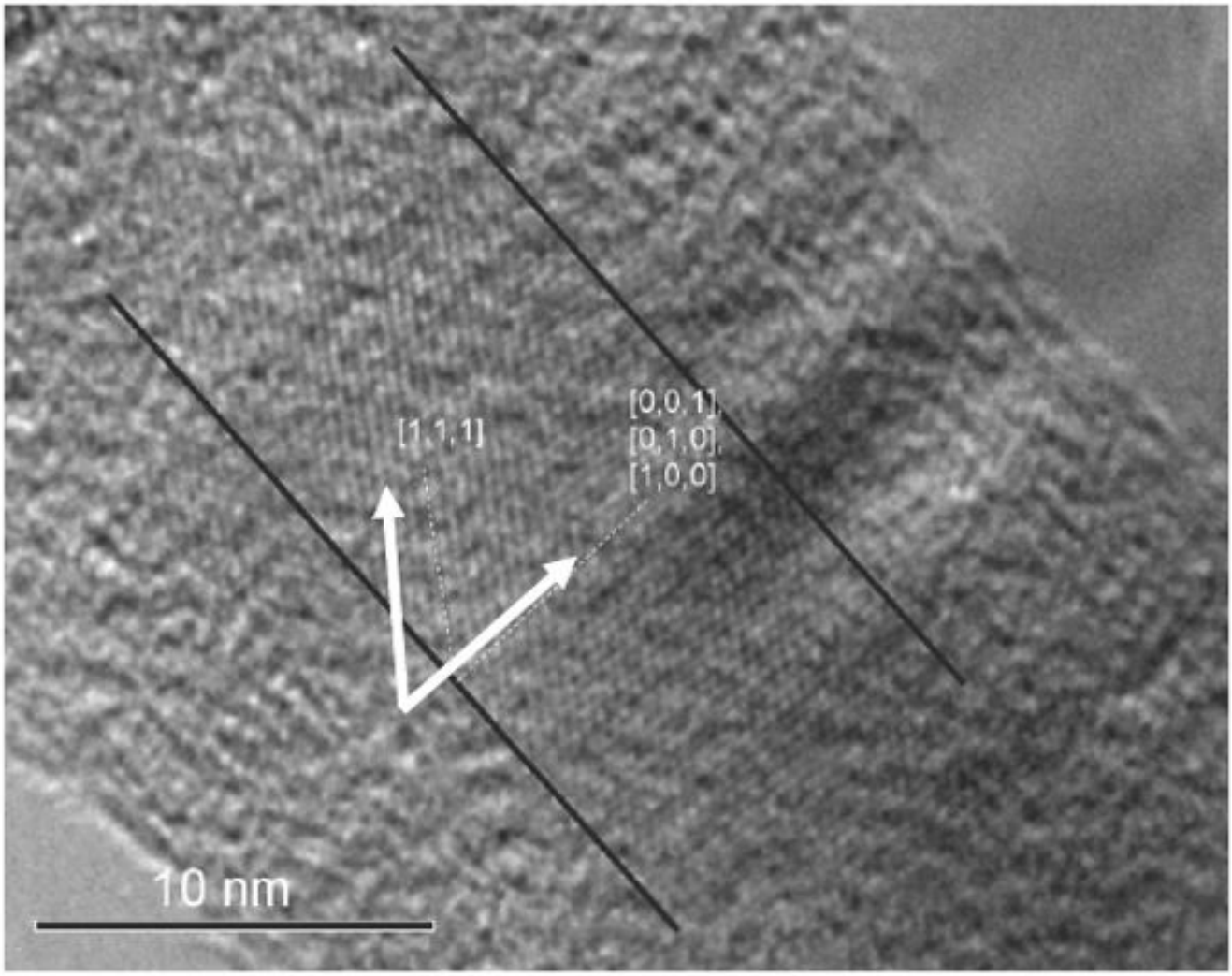

Figure 9.
HR-TEM of boron doped SiNW two years after synthesis. Note, the thick oxide layer (>8nm) and the Si core of 5-7 nm dimensions.

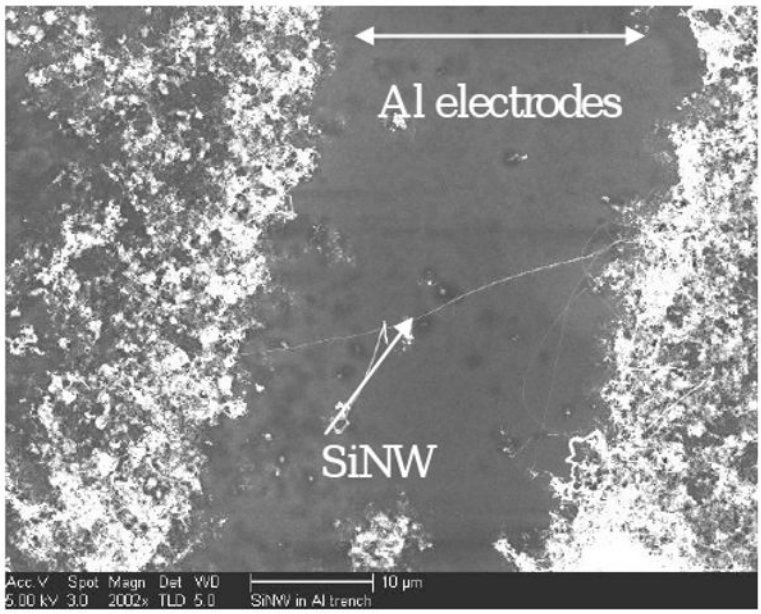

Figure 10.
A SEM image of capillary driven alignment and connection of Si-NW to Al electrodes. The details of the fabrication procedure are given in the experimental section.